



# Synthesis and Characterization of Fe/SBA-15 Heterogeneous Catalysts for Methyl Acetate Production

Veli Şimşek

Bilecik Seyh Edebali University, Chemical Engineering Department, 11210 Bilecik, Turkey (0000-0002-3518-1572) ([veli.simsek@bilecik.edu.tr](mailto:veli.simsek@bilecik.edu.tr)).

(1st International Conference on Applied Engineering and Natural Sciences ICAENS 2021, November 1-3, 2021)

(DOI:10.31590/ejosat.977591)

**ATIF/REFERENCE:** Şimşek, V. (2021). Synthesis and Characterization of Fe/SBA-15 Heterogeneous Catalysts for Methyl Acetate Production. *European Journal of Science and Technology*, (28), 21-28.

## Abstract

In the present study, the synthesis of SBA-15 (Santa Barbara Amorphous) support material (SPm) was initially carried out with the method determined according to the literature research. The catalytic property of SBA-15 was imparted by the hydrothermal method (HtM), different from the traditionally applied impregnation method. In this method, the active substance (iron III oxide;  $Fe_2O_3$ ) was added to the solution during the synthesis of the SPm. The amount of active substance in the synthesized catalysts was calculated based on the mass ratios of silicon (Si) in SBA-15 and iron (Fe) in  $Fe_2O_3$ . The active substance ratios in the catalysts were determined as 10, 25% Fe/Si. The activities of Fe/SBA-15 catalysts were tested in methyl acetate production (MAP). MAP reaction experiments were carried out in the presence of 0.4g catalyst (Fe/SBA-15), 373K, in autogenous pressure and 2/1 Acetic acid(AA)/methanol(MeOH) feed rate for 48 hours. The effects of active substance loading rate on AA conversion were determined. The structural properties of Fe/SBA-15 catalysts were investigated by XRD, BET, FTIR/DRIFT, SEM/EDX, and MAPPING analysis methods.

**Keywords:** Fe, SBA-15, Methyl acetate, Hydrothermal, Characterization.

## Metil Asetat Üretimi İçin Fe/SBA-15 Heterojen Katalizörlerin Sentezi ve Karakterizasyonu

### Öz

Sunulan bu çalışmada ilk olarak SBA-15(Santa Barbara Amorphous) destek maddesinin sentezi, literatür araştırmasına göre belirlenen yöntemle gerçekleştirilmiştir. SBA-15 maddesine katalitik özellik, geleneksel olarak uygulanan emdirme yönteminden farklı olarak, hidrotermal yöntemle(HtM) kazandırılmıştır. Bu yöntemde, aktif madde (demir III oksit ; $Fe_2O_3$ ) destek madde sentezi sırasında çözeltiliye eklenerek gerçekleştirilmiştir. Sentezlenen katalizörlerdeki aktif madde miktarı, SBA-15'teki silisyumun (Si) ve  $Fe_2O_3$  içerisindeki demirin (Fe) kütlece oranları baz alınarak hesaplanmıştır. Katalizörler içerisindeki aktif madde oranları %10, 25 Fe/Si olarak belirlenmiştir. Fe/SBA-15 katalizörlerin aktiviteleri, metil asetat üretiminde (MAÜ) test edilmiştir. MAÜ reaksiyon deneyleri, 373K, 0.4g katalizör(Fe/SBA-15) varlığında, otojenik basınçta ve 2/1 Asetik asit(AA)/metanol(MeOH) besleme oranında 48 saat boyunca gerçekleştirilmiştir. Aktif madde yükleme oranının AA dönüşümü üzerindeki etkileri belirlenmiştir. Fe/SBA-15 katalizörlerinin yapısal özellikleri ise XRD, BET, FTIR/DRIFT, SEM/EDX ve MAPPING analiz yöntemleriyle incelenmiştir.

**Anahtar Kelimeler:** Fe, SBA-15, Metil asetat, Hidrotermal, Karakterizasyon.

## 1. Introduction

Recently, the discovery by mobile researchers of silica-derived and metal-containing M41S materials, these materials have attracted the attention of scientists due to their mesopores, homogeneous pore size distribution, and high surface areas, both as a support for catalysts and as adsorption and separation (Şimşek, 2015). Their use as catalysts in fields attracts attention. Nowadays, silica-based support materials (SiBSMs) (such as SBA-15, SBA-16, MCM-41, and MCM-48) widely use synthesis of heterogeneous acidic catalysts (HeACs) (Şimşek, 2015; Şimşek & Avcı, 2018; Şimşek & Şahin, 2019).

Homogeneous acidic catalysts (HoACs) and HeACs are used in industrial-scale ester production. They used in the esterification reactions catalyze the reaction by giving a proton to the carboxylic acid (R-COOH) (Maki-Arvela et al., 1999; De Almeida et al., 2014). Homogeneous catalysts (HoCs) are generally used in esterification reactions (ERs) (Yin et al., 2013) such as HI (hydriodic acid), H<sub>2</sub>SO<sub>4</sub> (sulfuric acid), HCl (hydrochloric acid) and NaOH (sodium hydroxide), and (Yin et al., 2013; Helminen et al., 1998; Poonjarersilp et al., 2014; Oliviera et al., 2010). Recently, but, interest in heterogeneous catalysts (HeCs) has been intensified because HoCs dissolve quickly in the liquid reaction medium, cause corrosion, environmental pollution, do not easily decompose from the product, and require a separation process (Yin et al., 2013; Oliviera et al., 2010). for re-used. Among the SiBSMs, SBA-15 (Hess, 2009; Cavalleri et al., 2009) and M41S family (Brahmkhatri & Patel, 2011; Sawant, et al., 2007; Liu et al., 2004; Kumar et al., 2006) are the most well-known. Impregnation (Brahmkhatri & Patel, 2011; Sawant, et al., 2007; Liu et al., 2004; Kumar et al., 2006), dry-wet impregnation (Şimşek & Mürtezoğlu, 2019) and sol-gel (Yang, et al., 2005) methods are widely used in the synthesis of supported mesoporous materials and HeCs (solid catalysts). However, recently, direct HM has come to the forefront as an alternative synthesis method in studies where heteropoly acid catalysts (Fulvio et al., 2005) metals (Jimenez et al., 2010; Laugel et al., 2009) are used as active substances. Because HM has some advantages such as a homogeneous solution media for precursors, low material loss after synthesis procedure, low cost, and easy experiment properties or set up (Şimşek, 2019; Senapati & Maiti, 2020).

The sieve structure of SBA-15 has larger pore sizes and thicker pore walls compared to the M41S family (Şimşek, 2015; Thieleman et al., 2011). SBA-15 is a mesoporous silica sieve with adjustable pore diameters between 5 and 15 nm and a hexagonal structure with a narrow pore distribution. The fact that the wall frame thickness is between 3.1 and 6.4 nm is one of the main reasons for its higher hydrothermal and mechanical stability than materials such as MCM-41 (Thieleman et al., 2011).

SBA-15 is a suitable material for adsorption and separation in analytical environmental applications due to its high internal surface (400-900 m<sup>2</sup>/g) areas (Şimşek, 2015; Thieleman et al., 2011). It is also a suitable SPM in catalysts (Hess, 2009; Cavalleri et al., 2009; Şimşek, 2019). During the synthesis of SBA-15, which has a hexagonal mesoporous structure, it was observed that the pH value of the gel before washing with 300 ml of distilled water was always less than 0. After washing with

300 ml of distilled water, the pH value was obtained between 0-1. In other words, the pH value is very important for the catalytic activity of the SBA-15 SPM. The adjustable pore size in the synthesis of PMs increases the product selectivity. The pore size of the material must also be large then the large size of the organic molecules formed in the reaction. In catalyst synthesis, silica-alumina based materials are preferred because of that pore size ranges can be controlled depending on the synthesis parameters (Clark, 2002; Wilson & Clark, 2000).

Due to these properties, it is an important SPM for acidic catalysts used in ERs such as glycerol, which is obtained as a by-product in biodiesel production, and methyl acetate, ethyl acetate. The pH value before synthesis and after washing is important for the SBA-15 SPM to show high catalytic activity. ERs are equilibrium-limited and slow reactions. For this reason, there is a need for the use of catalysts in order to economically produce esters. Studies have shown that ester production increases in the presence of acidic homogeneous and heterogeneous catalysts (Röhnbak et al., 1997).

The heterogeneous catalysts used in the ER are usually homogeneously dispersed on a porous SPM. Natural or artificial solid materials, in which the pores are heterogeneously or homogeneously dispersed in different sizes and dimensions, are generally called porous materials. Their use as SPM in catalyst synthesis is one of the most important application areas of porous materials. The porous structure increases the surface area of the catalysts and increases their activity (Şimşek, 2008). The use of heterogeneous catalysts in ERs has increased in recent years. In reactions with heterogeneous catalysts, the parameters affecting the activity are temperature, stirring speed, catalyst amount, mole ratio of reactant, presence of inert material in the feed and retention time. The most important factors in the preference of solid acidic catalysts are that they reduce the corrosion problems and environmental problems that will occur due to the use of homogeneous acidic catalysts and do not create an additional separation cost in the chemical process (Helwani et al., 2009).

In this study, SBA-15 SPM synthesized by HM and Fe/SBA-15 (10,25% Fe/Si loading ratio) catalyst was synthesized. The catalytic activities of the synthesized materials (SBA-15, Fe/SBA-15) were tested in the MER selected as the model reaction. XRD, BET, FT-IR, DRIFTS, SEM/EDX, and MAPPING analysis methods were used to examine the structural changes of the synthesized materials before the reaction. The main purpose of this study is to investigate the synthesis, characterization, and catalytic activities of heterogeneous acid catalyst synthesized by the HM in the ER.

## 2. Material and Method

### 2.1. Synthesis of SBA-15 and Fe/SBA-15 Materials

SBA-15 synthesis was carried out in accordance with the synthesis procedure determined as a result of the literature search (Şimşek, 2019). Pluronic P123 as a surfactant, tetraethyl orthosilicate (TEOS) as silica source, deionized water (DW) as a solvent, and HCl acid for adjusting solution pH were used in the synthesis of porous material. First, pluronic P123 was dissolved in DW and stirred for 4 hours at 40°C until the solution became clear. Then, TEOS was added to the prepared clear solution. Within the scope of the study, the TEOS/Pluronic P123 ratio was

determined as “2”. After mixing for 2 hours, the solution obtained was placed in an autoclave and kept in an oven at 100°C for 48 hours. Second, the product, which became a gel in the autoclave, was washed with DW and a solid product was obtained after filtration. The solid product was then dried at 80°C for 12 hours. Finally, the sample was calcined at 540°C for 5 hours in order to remove the Pluronic p123 remaining during the synthesis in the SBA-15 structure. The HM was used in the synthesis of the Fe/SBA-15 catalyst used in the study. According to this method, TEOS was first added to the surfactant simultaneously with the active substance Fe<sub>2</sub>O<sub>3</sub>. The steps the solution goes through until it becomes solid are the same as for SBA-15 synthesis. Unlike the SBA-15 synthesis, the calcination temperature in the Fe/SBA-15 synthesis was determined as 350°C, taking into account the catalyst strength. The active substance ratio in the Fe/SBA-15 catalyst was determined based on the molar ratio of iron (Fe) in the iron (III) oxide structure to silicon (Si) in the TEOS structure. Within the scope of the study, this rate is Fe/Si: 10,25 %. The synthesis steps of the Fe/SBA-15 catalyst are shown schematically in Figure 1.

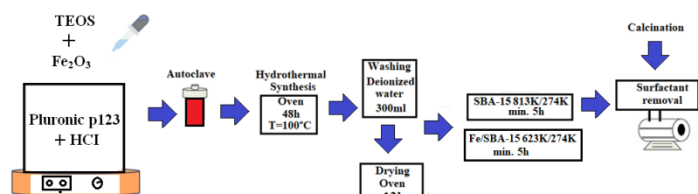


**Figure 1.** Synthesis procedures of SBA-15 SPM and Fe/SBA-15 catalyst.

## 2.2. Product of Methyl Acetate

The ERs were carried out in a batch reactor at autogenic pressure. The amount of Fe/SBA-15 catalyst was determined as 0.4g, the stirring speed was determined as 1000 rpm, and the mole ratio of AA/MetOH was determined as 2/1 during the experiments carried out in a reactor with methyl acetate production. Samples were taken at certain time intervals during the reaction and analyzed using Shimadzu gas chromatograph (GC-2010) instrument. In the gas chromatograph(GC) operation conditions are given in Table 1. MetOH and AA reactants with ethyl acetate synthesis and acetic acid conversion (Eq.1-2.)

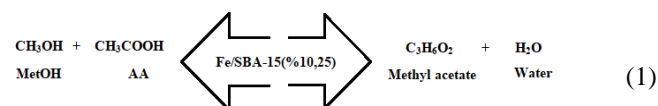


**Table 1.** Operation properties of GC[22].

Column	TRB Wax, 30mx0.32mmx0.5 µm Capillary column
Detector	FID (flame ionization detector)
Carrier gas and flow rate	N <sub>2</sub> (99.9%), 1.5 ml/min.
Column operated temperatures	80°C (1 minute) $\xrightarrow{15^{\circ}\text{C}/\text{min.}}$ 330°C (2 minutes)
Detector temperature	380 °C
Injection temperature	280 °C

$$XA =: \frac{AC*\alpha AC}{AC*\alpha AC+AB*\alpha AB+AA*\alpha AA} \quad (2)$$

Here: The AAC(%) is  $X_{AA/MtAC}$ , the calibration factor of methyl acetate is  $\alpha_{MtAC}$ , the calibration factor of MetOH is  $\alpha_{MtOH}$ , the calibration factor of AA is  $\alpha_{AA}$ , the area of methyl acetate is  $A_{MtAC}$ , the area of MetOH is  $A_{MtOH}$  and  $A_{AA}$  is the area of AA.

## 2.3. Characterization studies

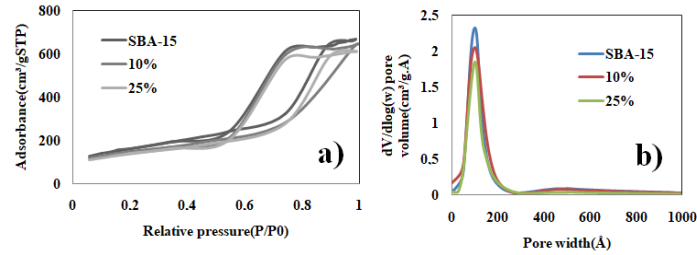
Fourier transform infrared spectroscopy(FT-IR) analyses of SBA-15 SPM and Fe/SBA-15 catalysts(10,25%) were performed using Perkin Elmer IR device between 380-4000 cm<sup>-1</sup> wavelengths. In order to determine the Brønsted acid acidity of the Fe/SBA-15 catalysts, multiple internal reflection(DRIFT) analyses were carried out using the pyridine(C<sub>5</sub>H<sub>5</sub>N) adsorbed samples in the same instrument and wavelength range, and the acid sites of the catalyst were determined. X-ray diffraction(XRD) analyses to identify structural phases of SBA-15 and Fe/SBA-15 catalysts: Panalytical Empyran HT-instrument; using CuKα radiation, 0.066 step pitch (sensitivity) and between 0°<2 θ<60° range were performed. In order to determine the surface area(SA), pore size distribution(PSD), and average pore distribution, multi-point Brunauer-Emmett-Teller(BET) and Barrett-Joyner-Halenda(BJH) analyses methods were carried out using the ASAP2020 device in the range of N<sub>2</sub> gas and 363-523K degas temperature for 3hours. The surface morphologies of the SPM and catalyst were determined by SEM/EDX (scanning electron microscope/energy dispersive x-ray, Zeiss SUPRA V40 instrument) analysis. Moreover, the MAPPING analysis method was used to determine the distributions of Fe and Si elements in the catalyst and support structure.

N <sub>2</sub> constant pressure	(58,0 kPa)
Hydrogen (H <sub>2</sub> )	(99.9%)
Dry air	(99.9%)
Injection sample volume	0.2µl

### 3. Results and Discussion

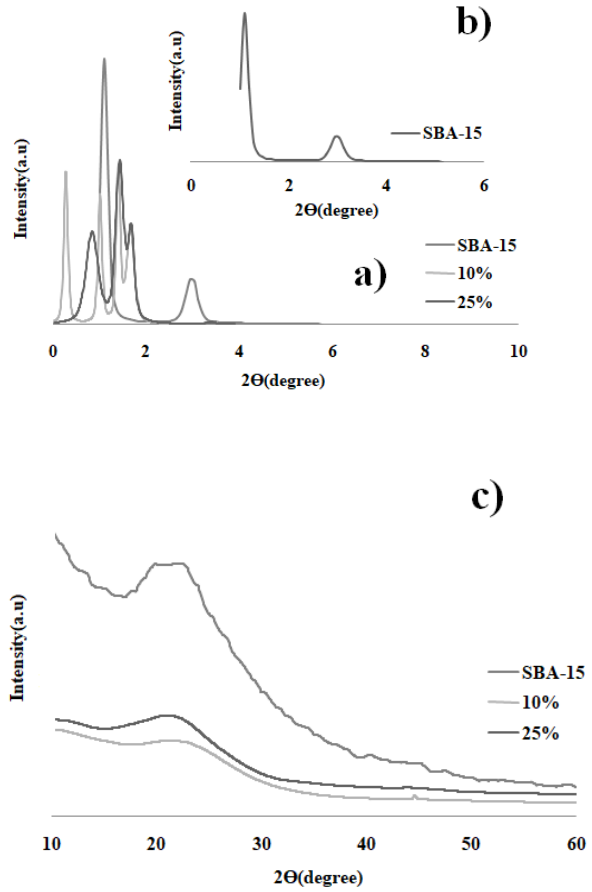
#### 3.1. Characterization Analyses

Figure 2 (a) shows N<sub>2</sub> adsorption/desorption experiments of SBA-15 SPM and Fe/SBA-15 (10, 25% Fe:Si). And BJH pore volume distribution is given in Fig 2(b). SBA-15 and 10, 25% catalysts have shown a type IV isotherm curve with an H1 hysteresis loop its characteristic of mesoporous structure[30]. The surface area and pore volume decreased as a result of the addition of Fe<sub>2</sub>O<sub>3</sub>. These reductions are thought to be due to the accumulation of Fe<sub>2</sub>O<sub>3</sub> on the pore walls, as well as some of it entering the pore. Changes in the structure of the 10% Fe/SBA-15 catalyst can be explained by the changes in the SBA-15 structure of the Fe added to the structure rather than the reaction effect.



**Figure 2.** a) BET isotherm curves, and b) BJH desorption pore volume distribution of materials.

Figure 3 shows SBA-15 has a regular mesoporous and hexagonal structure(Şimşek & Avcı, 2018; Helwani et al., 2009; Huang et al., 2010; Baskarana et al., 2014) with d100, d110 main peaks(Quach et al.,2020). Furthermore, in the characteristic peaks of SBA-15 SPM were observed shifts and losses after loading Fe(Figure 3)(Şimşek, 2015; Şimşek, 2019; Baskarana et al., 2014). According to the XRD analysis results of the SBA-15 SPM, it was observed that Bragg peaks at 1.12° and 2.94° 2θ values were obtained. Moreover, the characteristic peaks of SBA-15 were obtained in accordance with the literature(Şimşek, 2015; Şimşek, 2019) Figure 3(a). Although there were shifts in the basic Bragg peaks of SBA-15 after the active substance loading, 200 and 210 peaks were observed Figure 3(a,b) (Magdalena et al., 2019). It was assumed that this was due to the fact that the active substance did not cause significant changes in the structure during synthesis. As expected, no significant changes were observed in wide-angle XRD analyses (Figure 3(c)). These results are supported by the SEM analysis image of the Fe/SBA-15 catalyst before the reaction (Figure 6,7).



**Figure 3.** XRD analyses(low angle (a,b) and c) high angle) of SBA-15 and Fe/SBA-15(10,25%) materials.

**Table 2.** Physical properties of SBA-15 and Fe/SBA-15(10, 25%) materials.

Material	BET surface area(m <sup>2</sup> /g)	Pore volume (cm <sup>3</sup> /g)	Micro surface area (m <sup>2</sup> /g)	Average pore diameter(d p) (Å)	d(100) (nm)	Lattice parameters (a:nm)
SBA-15	636.7	1.27	48.6	95.4	8.85	9.87
Fe/SBA-15*	537.5	1.07	36.8	103.5	8.14	9.38
Fe/SBA-15**	289.4	0.40	14.4	112.7	7.76	8.96

\*10% Fe/Si, \*\*25% Fe/Si

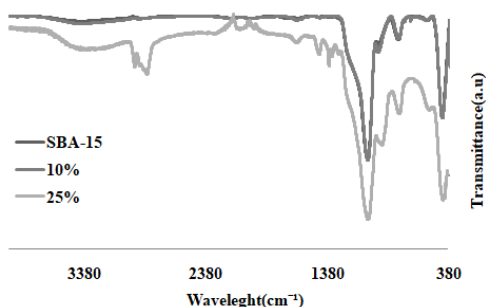
The characteristic lattice parameters "a" of SBA-15 and 10,25% catalysts were obtained using Eq. (3) "a=2d<sub>(100)</sub>/3<sup>1/2</sup>". The lattice and d(100) parameters of materials were measured using BET and XRD analyses methods.

$$a = 2d(100)/\sqrt{3} \tag{3}$$

Here: a; lattice parameters, d(100): dspace(distance between planes).

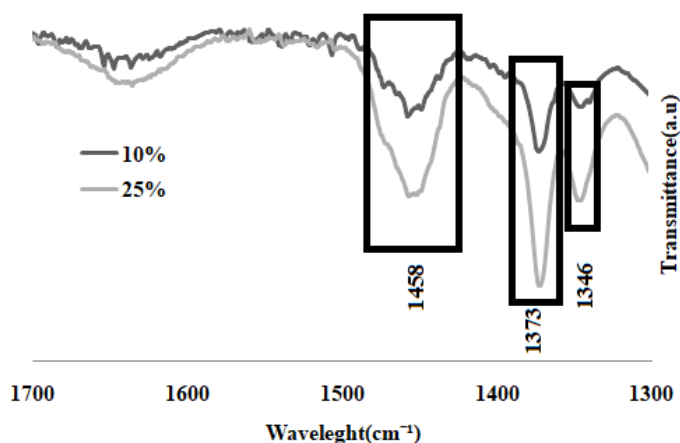
Figure 4 illustrates FTIR analysis results of SBA-15 SPM and Fe/SBA-15 catalysts. 447-1045cm<sup>-1</sup> wavelengths indicate SBA-

15 characteristic structure peaks. Si-O and SiO<sub>2</sub> tensile and flexible vibrations (symmetrical and asymmetrical) peaks of it were obtained 1045, 940, 787cm<sup>-1</sup> wavelengths, respectively (Junhong et al., 2020). Moreover, the 447cm<sup>-1</sup> peak corresponds to Si-O-Si bending vibration in the structure of SBA-15 (Bhuyan et al., 2017).



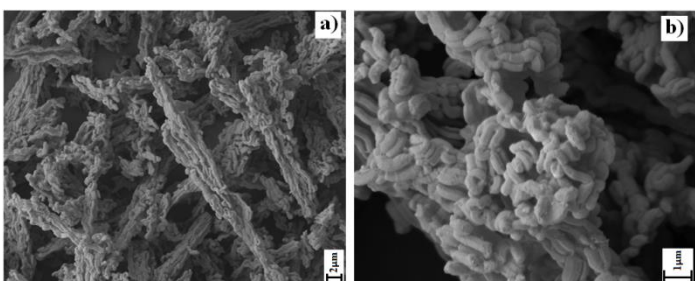
**Figure 4.** FTIR analyses of SBA-15 and Fe/SBA-5 (10,25%) materials.

Figure 5 shows DRIFT analyses peaks of Fe/SBA-15 (Fe/Si:10,25%) catalysts. Lewis acid site (LeAs) and Brønsted acid site (BrAs) was obtained at between 1300-1500cm<sup>-1</sup> wavelengths (Figure 5). LeAs and BrAs site of Fe/SBA-15 (Fe/Si:10,25%) catalysts were obtained at 1347-1346, 1458-1458 cm<sup>-1</sup> wavelengths, respectively (Cavlar et al., 2007). 1372 and 1373 peaks corresponded to pyridine physically adsorbed in the catalyst structure (Cavlar et al., 2007).



**Figure 5.** Drift analyses of Fe/SBA-15 (10,25%) materials.

The p6mm space groups and wheat structures of the SBA-15 SM (Thieleman et al., 2011) were indicated in the SEM analysis results (Fig.6,7 (a, b)). Moreover, these structures were preserved after active compound (Fe) loading (Fig.6,7(a,b)). The results of SEM/EDX and MAPPING analyses, it was determined that the distribution of Fe and Si elements on the support material (SBA-15) surface was homogeneous (Fig.8,10;a,b). The EDX results of catalysts indicated that the increase in the amount of Fe (active compound) loading in the SBA-15 has been proven (Fig.9,11).



**Figure 6.** SEM images of parent Fe/SBA-15 (10% Fe/Si ; a, b; 5-20kx).

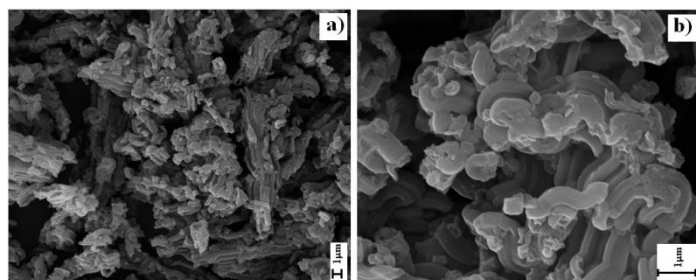


**Figure 7.** SEM images of parent Fe/SBA-15 (25% Fe/Si ; a, b; 5-20kx)

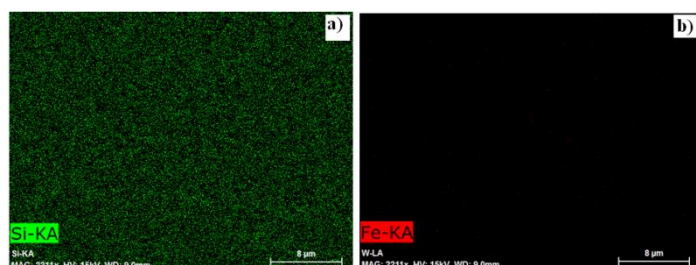


**Figure 8.** MAPPING images of parent Fe/SBA-15 (10% Fe/Si ; 2.211kx).

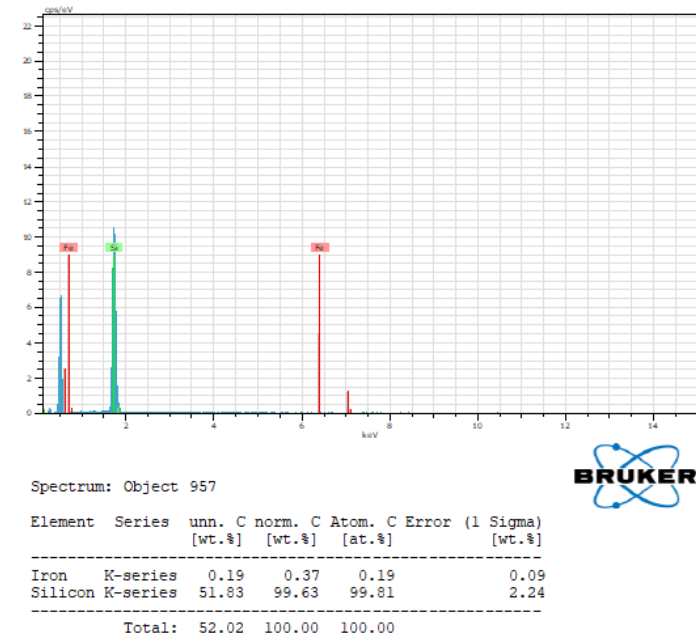


**Figure 9.** EDX analysis of parent Fe/SBA-15 (10% :Fe/Si).

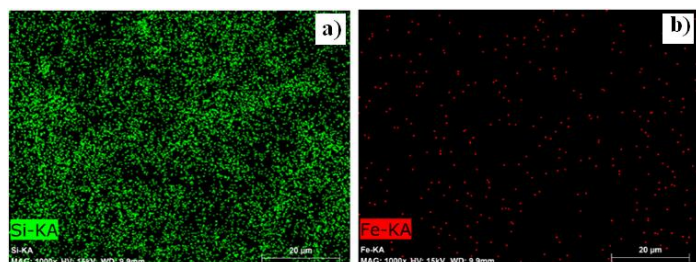


**Figure 10.** MAPPING images of parent Fe/SBA-15 (25% Fe/Si ; 1kx).

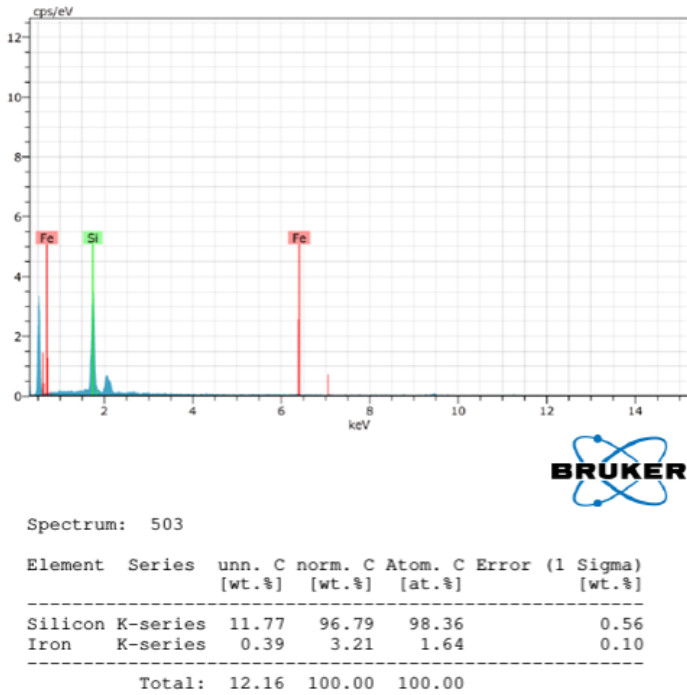


Figure 11. EDX analysis of parent Fe/SBA-15 (25% : Fe/Si).

### 3.2. Catalytic Analyses

Catalytic activities of synthesized Fe/SBA-15 catalysts within the scope of the study; It was investigated by methyl acetate synthesis with MetOH and AA reactants at 373 K. Reaction experiments were carried out in a batch reactor. Experiment conditions have been determined as catalyst amount of 0.4g, stirring speed of 1000 rpm, the mole ratio of AA/MetOH 2/1, and analysis time 48 hours. AA conversion values were obtained as 43-48, 55-61 and 64-72%, respectively after 6, 24 and 48hours(Fig. 12(a,b,c)). However, the reaction was not reached to balance limitation. On the other hand, the initial reaction rates of catalysts at different temperatures were calculated. The calculations were obtained at the end of 1 hour and using the batch reactor equation. Parameters: Volume of the batch reactor; V, and V=V0(volume batch reactor=initial volume). the IRR (initial reaction rates), and the SRR(specific reaction rate) of Fe/SBA-15 catalysts( %10,25) are shown in Table 3.

Table 3. IRR and SRR values of Fe/SBA-15 catalysts( %10,25).

Materials	Temperature (K)	SRR (k;L/mol.min)	IRR(-rA) mol/L.min
Fe/SBA-15*	373	$1.159 \times 10^{-4}$	0.013459
Fe/SBA-15**	373	$1.27 \times 10^{-4}$	0.014525

\*10% Fe/Si, \*\*25% Fe/Si

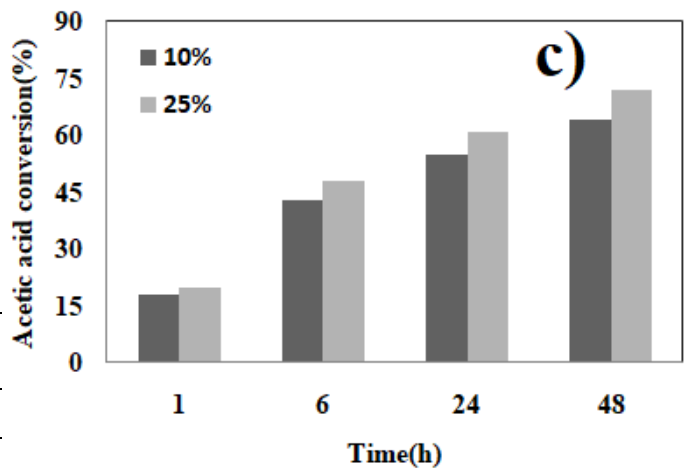
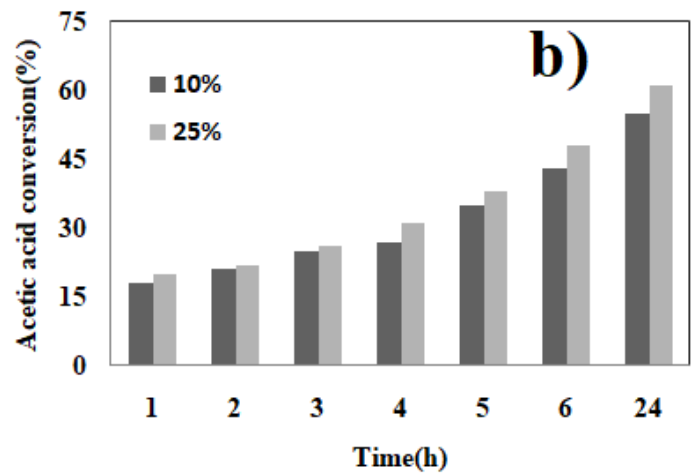
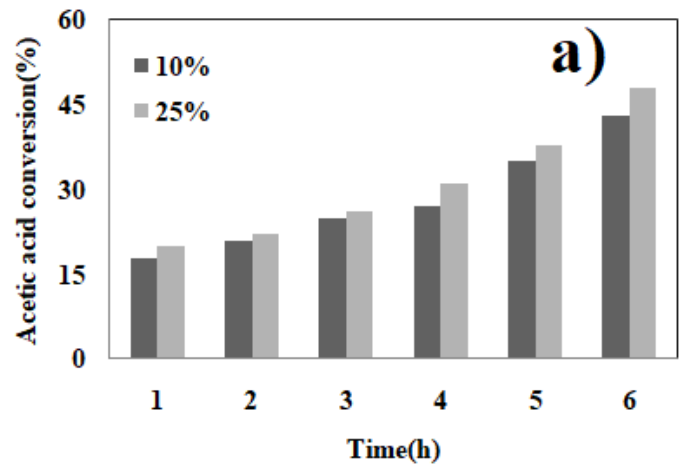


Figure 12. Acetic acid conversion (a)6h, (b)24 and (c) 48h.

## 4. Conclusions and Recommendations

SBA-15 SPM and Fe/SBA-15 catalysts were successfully synthesized with HM. Moreover, the characterization studies carried out on the materials proved that the synthesis of SBA-15 was carried out successfully in accordance with the literature. By the way, it was observed that Fe added to the structure during the synthesis not caused structural deterioration in the Fe/SBA-15 catalyst.

By adjusting the synthesis conditions, the active substance was homogeneously added to the catalyst structure and the activity of the catalyst was adjusted depending on the parameters applied in the synthesis procedures. Catalytic activity values of 10, 25% catalysts were calculated as 64 and 72%, respectively after 48 hours.

It is estimated that Fe/SBA-15 catalysts synthesized by the HM will be more efficient in higher temperature reactions. This is because the SBA-15 SPM has high thermal stability and thick wall thicknesses.

## References

- Baskarana, T., Christopher, J., Ajithkumar, T.G., Sakthivel, A. (2014). SBA-15 intercalated Mg–Al hydrotalcite: An environmental friendly catalyst for hydroisomerization of olefin. *Applied Catalysis A: General*, 488, 119-127.
- Bhuyan, D., Selvaraj, K., Saikia, L. (2017). Pd/SBA-15 nanocomposite catalyst: Synthesis and efficient solvent-free semihydrogenation of phenylacetylene under mild conditions, *Microporous and Mesoporous Materials*, 241, 266-273.
- Brahmkhatri, V., Patel, A. (2011). 12-Tungstophosphoric acid anchored to SBA-15: An efficient, environmentally benign reusable catalysts for biodiesel production by esterification of free fatty acids. *Applied Catalysis A: general*, 403, 161-172.
- Cavalleri, M., Hermann, K., Knop-Gericke, A., Havecker, M., Herbert, R., Hess, C., Oestereich, A., Döbler, J., Schlögl, R. J. (2009). *Catal.*, 262, 215-223. Doi:10.1016/j.jcat.2008.12.013.
- Clark, J.H. (2002). Solid acids for green chemistry. *Acc. Chem. Res.*, 35:791-797.
- Cavlar, N., Gonzalez, B., Dominguez, A. (2007). Esterification of acetic acid with ethanol: Reaction kinetics and operation in a packed bed reactive distillation column. *Chemical Engineering and Processing*, 46, 1317-1323.
- De Almeida, R. M., Souza, F. T. C., Junior, M. A. C., Albuquerque, N. J. A., Meneghetti, S. M. P., Meneghetti, M. R. (2014). Improvements in Acidity for TiO<sub>2</sub> and SnO<sub>2</sub> via Impregnation with MoO<sub>3</sub> for the Esterification of Fatty Acids, *Catalysis Communications*, 46, 179-182.
- De Sousa, F. F., Oliveira, A. C., Filho, J. M., Pinheiro, G. S., Giotto, M., Barros, N. A., Souza, H. S. A., Oliveira, A. C. (2013). Metal oxides nanoparticles from complexes on SBA-15 for glycerol conversion. *Chemical Engineering Journal*, 228, 442-448.
- Fulvio, P. F., Pikus, S., Jaroinc, M. (2005). Short-time synthesis of SBA-15 using various silica sources. *Journal of Colloid and Interface Science*, 287, 717-720.
- Helminen, J., Leppamaki, M., Paatero, E., Minkkinen, P. (1998). Monitoring the Kinetics of the Ion –Exchange Resin Catalysed Esterification of Acetic Acid with Ethanol Using Near Infrared Spectroscopy with PLS Model, *Chem. Int. Lab. Sys.*, 44, 341-352.
- Helwani, Z., Othman, M. R., Aziz, N., Kim, J., Fernando, W. J. N. (2009). Solid heterogeneous catalysts for transesterification of triglycerides with methanol. *Applied Catalysis A: General*, 363, 1-10.
- Hess, C. (2009). *Chem Phys Chem.*, 10, 319-326. Doi:10.1002/cphc.200800585.
- Huang, H., Ji, Y., Qiao, Z., Zhao, C., He, J., Zhang, H. (2010). Preparation, characterization, and application of magnetic Fe-SBA-15 mesoporous silica molecular sieves, *Journal of Automated Methods and Management in Chemistry*, doi:10.1155/2010/323509, 2010.
- Jimenez, M.I., Gonzalez, J.S., Torres, P.M., Lopez, A.J. (2010). Zirconium doped MCM-41 supported WO<sub>3</sub> solid acid catalysts for the esterification of oleic acid with methanol. *Applied Catalysis A: General*, 379, 61-68.
- Junhong, W. J., Shao, X., Liu, J., Ji, X., Ma, J., Tian, G. (2020). Fabrication of CdS-SBA-15 nanomaterials and their photocatalytic activity for degradation of salicylic acid under visible light, *Ecotoxicology and Environmental Safety*, 190, 110139.
- Kumar, G. S., Vishnubharth, M., Palanichamy, M., Murugesan, V. (2006). SBA-15 supported HPW: Effective catalytic performance in the alkylation of phenol. *Journal of Molecular Catalysis A: Chemical*, 260, 49-55.
- Laugel, G., Arichi, J., Bernhardt, P., Moliere, M., Kennemann, A., Garin, F., Louis, B. (2009). Preparation and characterisation of metal oxides supported on SBA-15 as a methane combustion catalysts. *C. R. Chimie*, 12, 731-739.
- Liu, Q.Y., Wu, W. L., Wang, J., Ren, X. Q., Wang, Y. R. (2004). Characterization of 12-tungstophosphoric acid impregnated on mesoporous silica SBA-15 and its catalytic performance in isopropylation of naphthalene with isopropanol. *Microporous and Mesoporous Materials*, 76, 51-60.
- Magdalena, P., Jacek, Z., Adrian, S., Adrianna, S., & Gavin, W. (2019). Surface-Activated Fibre-Like SBA-15 as Drug Carriers for Bone Diseases. *AAPS PharmSciTech* 20: 17 DOI: 10.1208/s12249-018-1243-5.
- Maki-Arvela P, Salmi T, Sundell M, Ekman K, Peltonen R, Lehtonen J (1999) Comparison of Polyvinylbenzen and Polyolefin Supported Sulphonic Acid Catalysts in the Esterification of Acetic Acid, *Applied Catalysis A: General*, 184, 25-32.
- Oliviera, C. F., Dezaneti L. M., Garcia, F. A. C., DeMacedo, J. L., Dias, J. A., Dias, S. C. L., Alvim, K. S. P. (2010). Esterification of Oleic Acid with Ethanol by 12-Tungstophosphoric Acid Supported on Zirconia, *Applied Catalysis A: General*, 372, 153-161.
- Poonjarersilp, C., Sano, N., Tamon, H. (2014) Hydrothermally Sulfonated Single-Walled Carbon Nano Horns for Use as Solid Catalysts in Biodiesel Production by Esterification of Palmitic acid", *Applied Catalysis B: Environmental*, 147, 726-732.
- Quach, N. K. N., Nguyen, T. Y., Nguyen, D. H., & Hoai, L. T. (2020). Synthesis and Characterization of Mesoporous Silica SBA-15 and ZnO/SBA-15 Photocatalytic Materials from the Ash of Brickyards. *Journal of Chemistry*, vol.2020. ID456194, 8 pages, 2020. <https://doi.org/10.1155/2020/456194>
- Röhnback, R., Salmi, T., Vuori, A., Hoorio, H., Lehtene, J., Sundquist, A., Tirronen, E. (1997). Development of a kinetic model for the esterification of acetic acid with methanol in the presence of a homogenous acid catalyst. *Chemical Engineering Science*, 52: 3369 -3381.

- Sawant, D. P., Vinu, A., Justus, J., Srinivasu, P., Halligudi S. B. (2007). Catalytic performances of silicotungstic acid/zirconia supported SBA-15 in an esterification of benzyl alcohol with acetic acid. *Journal of Molecular Catalysis A: Chemical*, 276, 150-157.
- Senapati, S., & Maiti, P.(2020). Emerging bio-applications of two-dimensional nanoheterostructuree materials, *2D Nanoscale Heterostructured Materials* 243-255. di:10.1016/b97-0-12-17678-8.00009-9.
- Şimşek, V. (2015). Synthesis, characterization and investigation catalytic activity in the glycerol esterification reaction of acidic catalyst, *Ph.D. Thesis*, Gazi university graduate school of natural and applied sciences, January Turkey.
- Şimşek, V., & Avcı, P.(2018). Characterization and Catalytic Performance of Modified SBA-16 in Liquid Phase Reaction, *International Journal of Chemical Reactor Engineering*. 2018.16(8): DOI: <https://doi.org/10.1515/ijcre-2017-0246>.
- Şimşek, V., Şahin, S. (2019). Characterization and catalytic performance evaluation of a novel heterogeneous mesoporous catalyst for methanol-acetic acid esterification. *Journal of Porous Materials*. May (2019) <https://doi.org/10.1007/s10934-019-00764-4>.
- Şimşek, V.(2019). Investigation of catalytic Sustainability of Silica-Based Mesoporous Acidic Catalysts and Ion-Exchange Resins in Methyl Acetate Synthesis and Characterizations of Synthesized Catalysts, *Arabian Journal for Science and Engineering*. 44, 5301–5310. <https://doi.org/10.1007/s13369-018-3570-y>.
- Simsek, V. (2008). Application of Mercury Porosimetry to Three Dimensional ( 3D) Stochastic Network Model and Researching Network Size Effect on Structure of Porous Media. *MSc Thesis*, Gazi univrsiy graduate school of natural and applied sciences January, Ankara.
- Şimşek, V., Mürtezoğlu, K.(2019) Investigation of lauric acid conversion with the STA incorporated heterogeneous catalysts in liquid phase reaction. *BSEU Journal of Science*, 6(1),91-103, DOI: 10.35193/bseufbd.553967.
- Thieleman, J. P., Girgsdies, F., Schlögl, R., Hess, C. (2011). Pore structure and surface area of silica SBA-15: Influence of washing and scale-up, *Beilstein Journal of Nanotechnology*, 2, 110-118.
- Wilson, K., Clark, J.H.(2000). Solid acids and their use as environmentally friendly catalysts in organic synthesis. *Pure Appl. Chem.*,72:1313-9.
- Yang, L., Qui, Y., Yuan, X., Shen J., Kim, J. (2005). Direct synthesis, characterization and catalytic application of SBA-15 containing heteropolyacid H3PW12O40. *Journal of Molecular Catalysis A: Chemical*, 229, 199-205.
- Yin, W.L.P., Liu, X., Chen, W., Chen, H., Liu, C., Qu, R., Xu, Q.(2013). Microwave Assisted Esterification of Free Fatty Acid over a Heterogeneous Catalyst for Biodiesel Production, *Energy Conversion and Management*, 76,1009-1014.